Acquisition and prediction of wave surface by marine radar for the safety of small ships

Hironori Susaki, *FURUNO ELECTRIC CO., LTD.*, hironori.susaki@furuno.co.jp
Yoshiaki Hirakawa, *Yokohama National University*, hirakawa-yoshiaki-jd@ynu.ac.jp
Takehiko Takayama, *Yokohama National University*, takayama-takehiko-yf@ynu.ac.jp
Tsugukiyo Hirayama, *Yokohama National University*, hirayama-tsugukiyo-nr@ynu.ac.jp

ABSTRACT

In recent years, wave observation by marine radar becomes increasing importance for the safety and the improvement of fuel efficiency of the ship. There are several wave radar systems for only wave observation and almost of wave radar systems for wave prediction are under development. The wave prediction is important especially for small ships, considering of stability by water on deck caused by a direct hits of wave. For avoiding direct hits of wave breaking, the authors attempts to predict encounter wave profile by utilizing a marine radar with a new algorithm based on the Fourier analysis and water wave dispersion relationship. Through the field experiments, the accuracy of wave observation verified by a wave buoy and the predicted wave surface shows good agreement with the actual wave surface.

Keywords: *Wave observation, Radar, Wavy buoy, Field experiments.*

1. INTRODUCTION

The research utilizing marine radars for wave observation started from 1975, it can be seen in the report by the Japan Ship Technology Research Association. It reported about the analysis to obtain the wave direction from PPI (Plan Position Indicator) images. After such a research, several wave radar systems were put to practical use, significant wave height, average period and directional distribution can be obtained by the wave radar systems.

YNU (Yokohama National University) group (Hirayama et.al.) started related research from 2000, and Nomiyama & Hirayama (2003) showed by numerical approach that individual waves can be obtained by PPI images and it opens the way for wave prediction in very short term (Nishimura & Hirayama et.al. (2004, 2005)). If incident waves can be predicted, ship motion also can be predicted. It leads to improvement of the ship safety and the energy saving navigation.

Especially for fishing vessels, smaller than cargo ships, prediction of incident waves will be very useful, for example, to avoid capsizing by waves. Table.1.1 shows an example of the distribution of the maximum rolling angle of a ship model by breaking wave hitting in the wave tank of YNU (Fig.1.1). From this it will be said that phase-difference information between the ship position and the wave is important. In this case, the height of the breaking wave is near the breadth of the ship. In this paper, the authors reported about the practical verification of wave observation and prediction utilizing marine radars by field experiments. Also, the theory of acquisition of ocean wave surface by a marine radar, verification by a wave buoy and examples of field experiments are reported.

Figure 1.1: The experiment for the breaking wave hitting

Table 1.1: Distribution of maximum rolling angle of fishing vessel by breaking wave hitting

		Heading Angle(deg)						
		45	60	75	90	105	120	135
Position from breaking point (mm)	800	32.66	43.76	48.09	45.43	43.06	44.78	28.09
	600	34.57	43.76	54.47	48.85	46.06	53.47	35.16
	400	32.76	42.03	51.11	50.29	48.00	45.86	29.81
	200	25.06	43.09	54.91	55.58	51.55	48.61	30.42
	0	24.64	29.18	40.90	51.11	45.96	40.22	26.66
	-200	22.88	23.08	25.54	41.45	27.87	29.54	23.37
	-400	20.40	19.33	25.49	24.86	21.19	26.15	20.06
	-600	21.13	23.85	24.32	24.41	24.94	22.41	24.00

2. THEORY

Strong intensity region of the image of a PPI is considered as the results of Bragg-Back-Scattering occurred in the ripples or white caps generated mainly by winds and these regions are also considered as existing around wave crests. But those intensities do not depend precisely on wave heights or wave slopes, so for the estimation of wave heights from PPI image we must develop other techniques.

First step is to obtain three dimensional Fourier spectrum (complex) for estimating power spectrum (real) of wave itself, eliminating noise part not relating to waves.

Here, ζ (x, y, t) is the density of PPI image and its three dimensional Fourier Spectrum F(kx,ky,ω) is obtained by equation (1) . F is complex, then decomposed as formula (2) using real part and imaginary part. From this, phase part of F is defined as formula (3).

$$F(k_x, k_y, \omega) = \int_{-\infty}^{\infty}\int_{-\infty}^{\infty}\int_{-\infty}^{\infty} \zeta(x, y, t).e^{-i(k_x \cdot x + k_y \cdot y + \omega \cdot t)}\, dxdydt \tag{1}$$

$$F(k_x, k_y) = F_{real}(k_x, k_y) + i \cdot F_{imag}(k_x, k_y) \tag{2}$$

$$\phi = \tan^{-1}\left(\frac{F_{imag}(k_x, k_y)}{F_{real}(k_x, k_y)}\right) \tag{3}$$

For eliminating the non-wave information in PPI-images, so called dispersion relation of gravity wave is introduced as a filter shown as equation (4).

Here vector U is ship speed, vector k is wave number, g is gravitational acceleration and ω is encounter frequency. ω -surface expressed by equation (4) is shown as Fig.2.1, and called as dispersion-shell (Borge et.al.(2000)).

$$\omega = \sqrt{g \times k} + \vec{k} \cdot \vec{U} \tag{4}$$

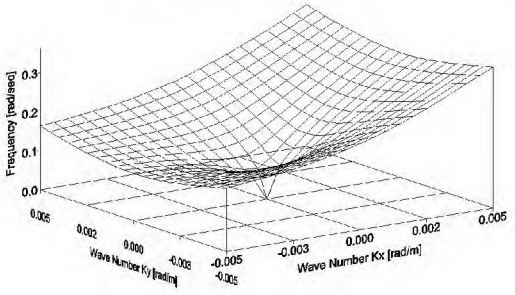

Fig.2.1 Example of the Dispersion Shell of surface wave (U=15knots)

Intensity of power spectrum of waves obtained by the product of F and F* (* means complex conjugate) also appear on the surface expressed as Fig.2.1, so, non-wave power is easily eliminated. From the power spectrum of wave, conventional information as significant wave height and mean wave frequency are estimated easily, by the volume and moment of spectrum as equation (5)~(8).

Here Lx, Ly, T are the size of analysing area of PPI image in x-y plane and time domain, P is directional spectrum in wave number , S is point spectrum in circular frequency , m_n is n-th moment, and T_{01} , T_{02} are mean periods defined by spectral moments. Fig.2.2 is an example of actual power spectrum appeared on the dispersion shell. Some fluctuations can be seen.

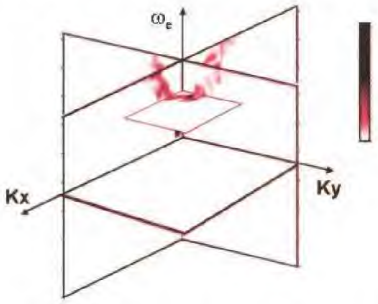

Fig.2.2 Example of power-spectrum-density over the dispersion shell.

$$P(k_x, k_y) = 2\,\frac{\int_{\omega>0} |F(k_x, k_y, \omega)|^2\, d\omega}{L_x \cdot L_y \cdot T} \tag{5}$$

$$S(\omega) = \int_{-\pi}^{\pi} P(\omega, \theta)\, d\theta \tag{6}$$

$$m_n = \int_0^{\infty} \omega^n \cdot S(\omega)\, d\omega \tag{7}$$

$$H_{1/3} = 4.01 \cdot \sqrt{m_0}$$

$$T_{01} = 2\pi \cdot \frac{m_0}{m_1} \tag{8}$$

$$T_{02} = 2\pi \cdot \sqrt{\frac{m_0}{m_2}}$$

Area for analysis

The intensity of PPI image of marine radar, affected by the strength and direction of winds over the sea surface, it is better that the area of analysis is chosen in the direction of winds coming, because

PPI-intensity become strong in the direction that wind is blowing from and not blowing to.

Decision of wave height

As already described, the intensity of PPI images including bias are not proportional to wave height ,so, the scale of vertical axis of power spectrum has some ambiguity. For resolving this problem, we introduced a method (patented) utilizing the monitoring ship motion (mainly heaving motion) spectrum and theoretical response amplitude operator between wave and motion.

3. FIELD EXPERIMENTS

The research ship "Taka-maru" (L_{OA}=29.5m) belonging to the NRIFE (National Research Institute of Fisheries Engineering, Japan), the training ship "Fukae-maru" (L_{OA}=49.95m, Kobe University, Japan) and the training ship "Shinyo-maru" (L_{OA}=60.0m, Tokyo University of Marine Science and Technology) are utilized for the field experiments. Wave radars are installed on each ship. Fig.3.1-3.3 show "Taka-maru", "Fukae-maru" and "Shinyo-maru". The red dotted circle in Fig3.1-3.3 shows the additional radar(s) specially for wave measurement.

For large ships, the height of additional radars are set as low as possible in order to reproduce the height-condition of small ships.

Figure 3.1: The research ship "Taka-maru"

Figure 3.2: The training ship "Fukae-maru"

Figure 3.3: The training ship "Shinyo-maru"

Wave observation by small buoys

To verify the result from the wave radar system, small buoys are developed and utilized. Conventional wave buoys are large, expensive and for long-term measurement. To realize small size (light), not so expensive and for short-term measurement, the "Ultra-Small-Directional-Wave-buoy" (Small-buoy) was developed by Hirayama et.al. The Small-buoy is mainly used in the field experiment utilizing "Taka-maru". After development of the Small-buoy the "Mini-buoy" was developed by Hirakawa et.al. (2003, 2016), because the field experiments utilizing "Fukae-maru" and Shinyo-maru" need smaller buoy.

Fig.3.4 shows the developed buoys for this research and principal dimensions of the buoys are shown in Table 3.1.

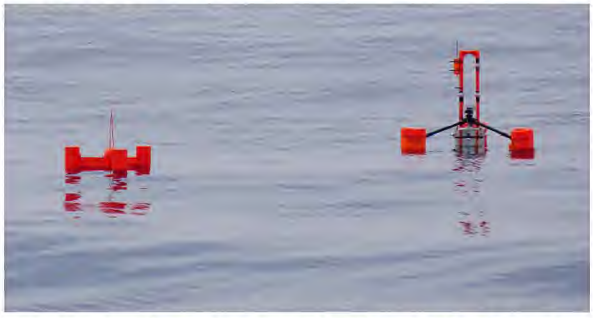

Figure 3.4: The Mini-buoy (Left) and the Ultra-Small-Directional-Wave-Buoy (Right)

Table 3.1: Principal Dimensions of the Mini-buoy and Ultra-small-directional-wave-buoy

	Mini-buoy	Small-buoy
Length of leg	0.3m	0.61m
Height from the bottom	0.3m	0.75m
Weight	4kg	13kg
Communication range	10m	600m
Time for recording	20hours	8hours

The motion of the buoy (height, period and direction) are measured and MLM (Maximum Likelihood Method) is utilized to calculate directional wave spectrum.

The measured vertical displacement using the sensors in Small-buoy was verified utilizing an image analysis method. As can be seen in Fig.3.5, markers for tracking is set on the buoy (2 points) and horizontal line (2 points). The time history of vertical displacement of the buoy shown in Fig.3.5 can be obtained. In Fig.3.6 the blue line shows the power spectrums of measured vertical displacement and the red line shows the power spectrum of wave calculated from the motion of image of the buoy.

The Mini-buoy was verified utilizing the experimental towing tank in YNU (Fig.3.7). The power spectrum of wave calculated from the motion of the buoy is compared with the power spectrum of wave measured by the wave probe in Fig.3.8.

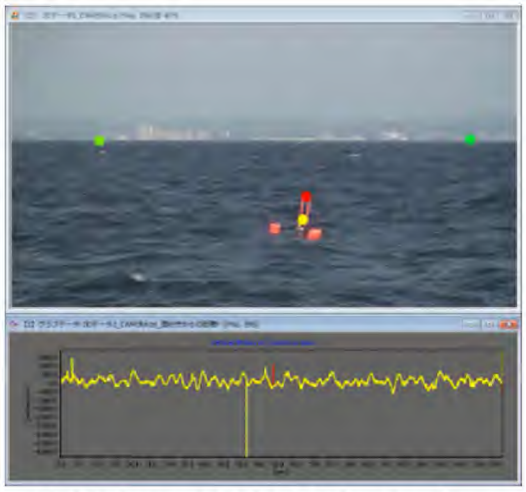

Figure 3.5: The image analysis of the buoy motion

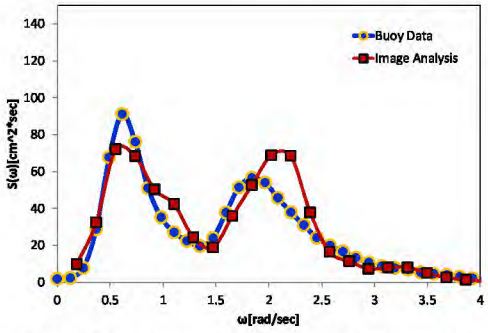

Figure 3.6: The power spectrum of measured vertical displacement of the buoy and analyzed data from the image of buoy motion.

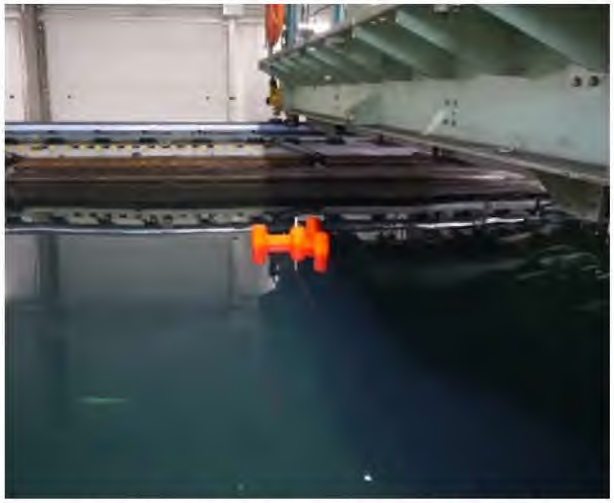

Figure 3.7: The verification experiment of the Mini-buoy in the experimental towing tank

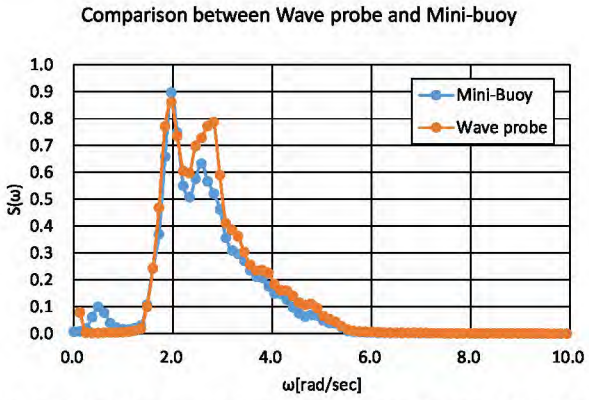

Figure 3.8: The power spectrum of wave by the Mini-buoy and the power spectrum of wave by the wave probe

Concrete example of wave observation by marine radar

We show an example of PPI image in Fig.3.9 (bow up drawing). This is obtained using commercial marine radar (DRS12A (4-feet antenna by Furuno). Rotation rate of antenna is 48rpm. Spectrum (Fig.3.10, north up drawing) is estimated using raw signal including back scatter from the sea surface and applying the method described in the

section 2. The observed date is Jun.14 2012 as shown in the Fig.3.9.

The range of PPI is 1500m, and the selected square area in this PPI for analysis is 1km by 1km. Wind coming direction is from the ship bow, so the selected area is also set in the direction of wind coming.

As can be seen from the spectrum, other than the main wave direction (wave 1), wave2 and wave3 seems exist as also shown in Fig.3.9.

In case of carrying out wave prediction (time history of surface elevation at the designated position and time), the phase part defined by the equation (3) is needed.

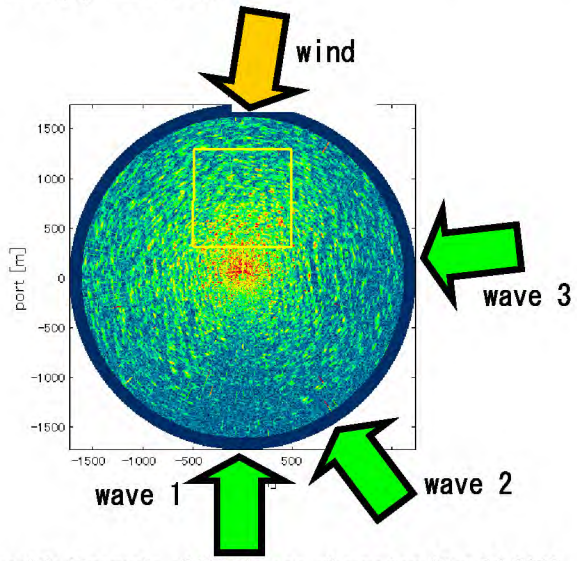

Figure 3.9: Example of PPI image of a radar (Jun.14 2012 12:46). Bow up expression.

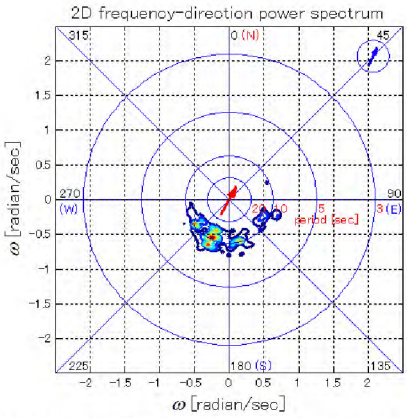

Figure 3.10: Example of obtained directional spectrum in frequency domain

Verification by wave buoy

The buoys are enough smaller than the wavelength and the motion of the buoys follow the slope and elevation of the wave surface. The directional distribution can be estimated from the motion of the buoy based on ergodic property. On the other hand, the radar can catch the total information of wave surface directly without the assumption of ergodicity, inside its range. So, the accuracy of directional characteristics by the radar is better than the buoys. From these kinds of reasons, wave height and period by the radar are verified by that by the buoy. Fig. 3.11 and 3.12 show the comparison between the radar and the buoy about the significant wave height and the average wave period. As can be seen in Fig. 3.11 and 3.12, the errors by the radar based on the buoy are plus or minus 7.0% in wave height and plus or minus 6.6% in wave period.

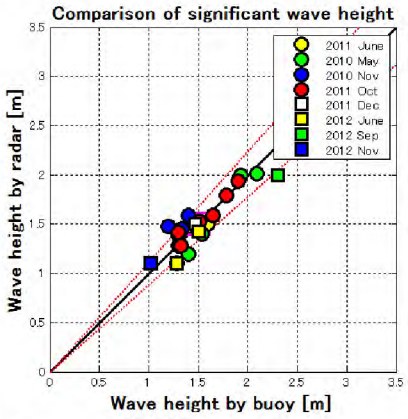

Figure 3.11 Comparison between radar and buoy from the past field experiments (Wave height)

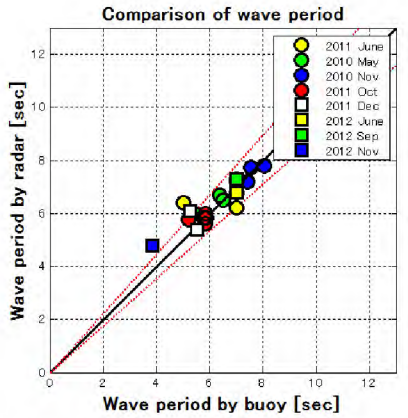

Figure 3.12 Comparison between radar and buoy from the past field experiments (Wave period)

Wave surface prediction

Watching the wave radar, we can know that the intensity of the surface back scatter moves with the wave speed. This means that the wave radar can detect the characteristics of surface wave. So, if we can obtain the accurate wave spectrum from PPI

image, then we can carry out the prediction of wave surface around the radar in relatively short time, 30sec, 60sec for example, and narrow area, 1km by 1km for example, according to the selected area by the wave radar. Prediction can be made changing the phase part of the spectrum according to the phase speed of component waves.

In case of predicting the wave surface (elevation map) by the Inverse Fast Fourier Transformation (IFFT), we need the following phase shift as equation (9) according to the time passing as Δt sec. The original phase $\phi(\omega(k),t)$ is given by equation (3).

By putting the wave buoy inside this map, then we can verify the accuracy of this prediction. Furthermore, by this method, we can predict the time-history of wave elevation at the desired point and time or that according to the trajectory of the moving ship.

$$\phi(\omega(k), t+\Delta t) = \phi(\omega(k), t) + \omega(k)\cdot\Delta t \qquad (9)$$

Those predictions will contribute to avoiding the meeting with dangerous situation for ships, especially small ships like fishing boat.

Test at sea cannot always meet with such a dangerous condition, so the useful cases are not enough, we show an example as follows.

This is the case carried out using the ship named Taka-Maru, already described, on 14th June 2012, at around the point of 34.92-laltitude and 139.61-longitude off Boso-peninsula near Tokyo. About this case, the ship is rested condition. Significant wave heights both from directional mini wave buoy and wave radar were about 1.8m.

Point wave spectrum from wave radar is shown in Fig.3.13. This is obtained integrating the Fig.3.10 in angular direction. Unit of abscissa is rad/s, and ordinate is relative power. Absolute power can be determined using monitored heaving motion of this ship as already described. From this determination, significant wave height is 2.03 m and mean wave period (T_{02}) is 8.47sec. So, it will be said that the swell is dominant.

Fig.3.14 show the time variant in 20-minutes of ship heading direction (□) and wave coming directions (△ show the primary or dominant wave, "○" show the secondary wave) estimated from the directional spectrum from wave radar. Ordinate range is 0-degree to 360-degrees. About wave direction, 0-dgree means wave coming from ship bow. 360-degrees fluctuations of ship heading occur from the 360 degrees-ambiguity of the definition of direction.

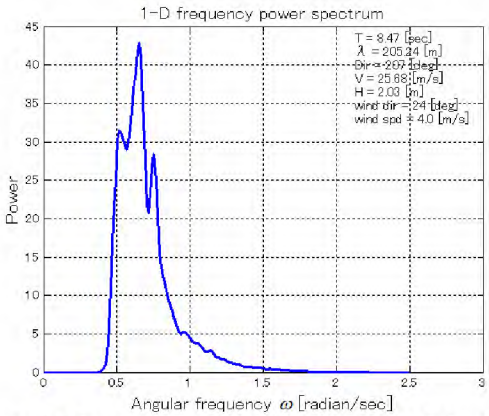

Figure 3.13: Example of point spectrum at 12:46 obtained from radar analysis. $H_{1/3}$=1.83m ,T_{02}=8.34sec, Wind Speed=3.0m/s

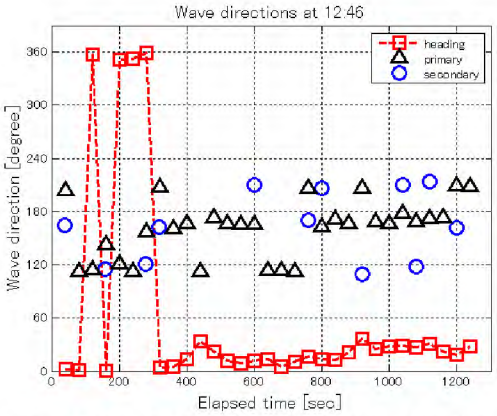

Figure 3.14: Change of the ship heading-angle(□), primary(Δ) and secondary(○) direction obtained from directional wave spectrum by wave radar, according to the time.

Fig.3.15 shows the comparison of predicted (left) and actual (right) wave map expressing surface elevation. Prediction is executed after 30 seconds from the initial time. In equation (9), Δt is put as 30sec for this case. Actual ones are the wave map obtained through the process of wave filter (equation (4)), corresponding to the time of the left figure. In short time, deviation of spectrum is small, then difference of significant wave height between predicted and actual one is small.

Usually, wave field cannot be obtained at the center part of PPI, namely near-radar position, but the wave map can be obtained at this center, because this map is obtained by the superposition of infinitely continuing long crested regular waves. This point seems superior point of this predicting method.

The numerals under each figure in Fig.3.15 show the rotated number of rotating antenna of the radar. The needed time for one rotation of this wave radar is 1.25 sec. Then, for example, 44 of 44(30)

means a predicted wave map using PPI image at the 44th rotation time and (30) means the predicted map at 30 seconds after. So, the rotation number at the predicted time become 68 from the started time. Numeral 68 of actual wave map in the right corresponds to the observed wave map at the rotation number is 68.

In the Fig.3.15, continuous prediction maps are shown, and in case of practical wave radar system, similar continuous renewals are shown in a display.

In this example, as the predictions are made in very short time, so the predicted wave maps seem relatively coincide with those of actual ones.

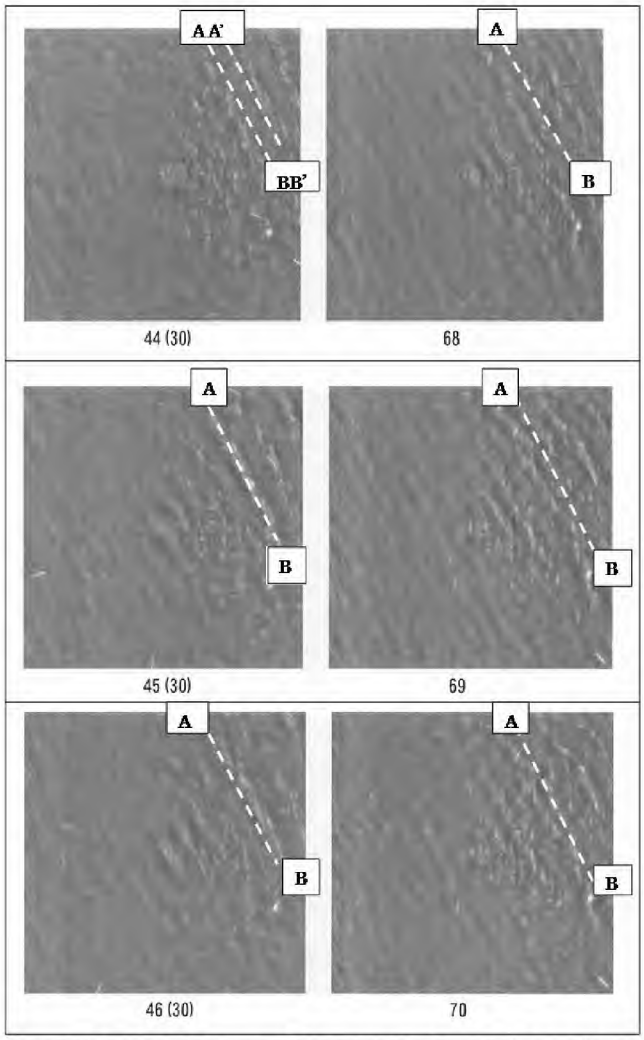

Figure 3.15: Comparison of the predicted wave fields after 30 seconds (left), and obtained wave fields by the radar after 30seconds (right). Numerals, 44 for example, means the number of the rotation of radar antenna. Inserted lines are reference line parallel to crest lines.

In order to evaluate more in details, we watch the movement of crest lines of waves. The period of dominant wave from wave spectrum is 8 seconds, the wavelength of this component wave is 99.8m, and the phase speed is 12.5m/s. This means that the crest of this wave moves about 16m (1/6 of wavelength) within the time of one rotation of radar antenna.

The inclined dotted line A B in the upper figure of Fig.3.15 is drawn parallel to wave crest line, and A'B' line is drawn by the space of one wave length. From those auxiliary lines, it can be seen that the wave map express tones corresponding to the crest lines of dominant wave. The same lines as this AB are drawn also in the following figures.

It can also be seen that the wave main direction of left and right wave map coincide with each other. Furthermore comparing with the upper, middle, bottom wave maps of the left column each other, it can be seen that the dominant wave moves to upper diagonal direction. This result also be seen in the actual wave map of the right column.

This means that if the wave at AB line is dangerous one, then we can alarm a ship approaching to the position of AB line, in 30 seconds ahead. Of course this alarm can be given to the own ship. Those comparisons must be made more for validating the accuracy of predictions.

4. CONCLUSIONS

The accuracy of wave height and period estimated by the wave radar are shown, they are plus or minus 7.0% in wave height and plus or minus 6.6% in wave period compared to wave buoys.

The practical example of very short term wave prediction is shown utilizing the extracted information of individual wave from PPI images by marine radar.

The analysis method of wave surface prediction utilizes the information of the individual wave including the phase, so the wave surface all over the position in the range even at the antenna position (namely ship position) can be estimated.

The verification experiment is not enough in case of rough sea condition as over 3m wave height. So, additional field experiments are needed.

ACKNOWLEDGMENT

The authors would like to thank Japan Science and Technology Agency (JST), the crews of Taka-maru, Fukae-maru and Shinyo-maru, the students of Kobe University, Tokyo University of Marine Science and Technology and Yokohama National

university and National Research Institute of Fisheries Engineering. We also express our appreciation to Mr. Reiji Nishikawa of YNU for his support to us. This work has been supported by JST.

REFERENCES

MIROS, "SM-050 Wave and Current Radar Mk III", http://www.miros.no/.

Chang-Kyu Rheem, 2007, "Water Surface Wave Observation by using Microwave Doppler Radar in Experimental Basin", *Journal of the Japan Society of Naval Architects and Ocean Engineers* 6, pp. 65-73.

Chang-Kyu Rheem, 2008, "Sea Surface Wave Observation by using CW Doppler Radar and Effect of Radar irradiation Width", *Journal of the Japan Society of Naval Architects and Ocean Engineers* 8, pp. 61-69.

Koji Nishimura, Tsugukiyo Hirayama, D.H. Nomiyama, Yoshiaki Hirakawa, Takehiko Takayama, 2004, "Navigation System for Dangerous-Wave-Avoidance Maneuver as an Application of Marine Radar and Motion Simulation Technique" Conference proceedings the Society of Naval Architects of Japan (4), pp.91-92.

Koji Nishimura, Tsugukiyo Hirayama, Takehiko Takayama, Yoshiaki Hirakawa, D.H. Nomiyama, 2005, "Unsteady Rolling Due to Turning Manoeuvre in Waves-II : Motion Simulation Based on Encounter Wave Prediction by Wave Radar", *The Journal of Japan Institute of Navigation* 112, pp. 307-314.

Tsugukiyo Hirayama, Yoshiaki Hirakawa, D.H. Nomiyama, Koji Nishimura, Takehiko Takayama, 2005, "On the distinction and prediction of encountering individual waves by the ship radar", Conference proceedings the Society of Naval Architects of Japan (5), pp. 87-88.

Nieto, Borge JC, Soares CG, 2000, "Analysis of directional wave field using X-band navigation radar", Coastal Engineering 40, pp. 375-391.

Takase Fabio K., Tsugukiyo Hirayama, 2000, "Evaluation of Marine Wave Radar(Part I) : Fundamental Considerations and Numerical Generation of Radar Image", *Journal of the Society of Naval Architects of Japan* (187), pp. 85-92.

Takase Fabio K., Tsugukiyo Hirayama, Park Seung Geun, 2000, "Evaluation of Marine Wave Radar (Part II) - Wave Parameters from Radar Images -", *Journal of the Society of Naval Architects of Japan* (188), pp. 225-237.

Tsugukiyo Hirayama, Park Seung Geun, Takase Fabio K, Kiyoshi Miyakawa, Takehiko Takayama, 2001, "Estimating method of surrounding-wave-characteristics utilizing marine radar", Conference proceedings the Japanese Society of Fisheries Engineering (13), pp. 147-150.

Tsugukiyo Hirayama, Park Seung Geun, Yoshiaki Hirakawa, , Takehiko Takayama, 2002, "Development of a Wave Field Detector using the Marine Radar and Measured Example", *Journal of the Society of Naval Architects of Japan* (191), pp. 51-56.

D.H. Nomiyama, Tsugukiyo Hirayama, 2003, "Numerical Simulation Applied to Real-time Ocean Wave Analysis : Wave radar", Conference proceedings the Society of Naval Architects of Japan (1), pp. 5-6.

D.H. Nomiyama, Tsugukiyo Hirayama, 2003, "Evaluation of marine radar as an ocean-wave-field detector through full numerical simulation", *Journal of marine science and technology* 8(2), pp.88-98.

D.H. Nomiyama, Tsugukiyo Hirayama, Takehiko Takayama, Yoshiaki Hirakawa, Koji Nishimura, Daigo Kabuto, 2003, "Wave-Field-Detection by the Marine Radar on a Small Ship", Conference proceedings the Society of Naval Architects of Japan, pp. 139-140.

Yoshiaki Hirakawa, Takehiko Takayama, Tsugukiyo Hirayama, Koji Nishimura, 2003, "Improvement of Directional-Wave-Mini-Buoy and Field Experiments", Conference proceedings Joint Autumn Meeting of Three Societies of Naval Architects in Japan, pp. 63-66.

Yoshiaki Hirakawa, Hironori Susaki, Seishi Sasaki, Takehiko Takayama, Akihiko Matsuda, Tsugukiyo Hirayama, 2015, "Acquisition of Ocean Wave Surface by X-band Ship Radar and Very-short-term Wave Surface Prediction", *Journal of the Japan Society of Naval Architects and Ocean Engineers* 22, pp. 235-242.

Yoshiaki Hirakawa, Takehiko Takayama, Tsugukiyo Hirayama, Hironori Susaki, 2016, "Development of Mini-Buoy for short term measurement of ocean wave", OCEANS 2016 MTS/IEEE Monterey.